

## Research Article

# Synthesis of Core-Shell $\text{Fe}_3\text{O}_4@\text{SiO}_2@\text{TiO}_2$ Microspheres and Their Application as Recyclable Photocatalysts

Zhenghua Wang, Ling Shen, and Shiyu Zhu

Anhui Key Laboratory of Functional Molecular Solids, College of Chemistry and Materials Science, Anhui Normal University, Wuhu 241000, China

Correspondence should be addressed to Zhenghua Wang, zhwang@mail.ahnu.edu.cn

Received 14 January 2012; Revised 2 March 2012; Accepted 2 March 2012

Academic Editor: Xuxu Wang

Copyright © 2012 Zhenghua Wang et al. This is an open access article distributed under the Creative Commons Attribution License, which permits unrestricted use, distribution, and reproduction in any medium, provided the original work is properly cited.

We report the fabrication of core-shell  $\text{Fe}_3\text{O}_4@\text{SiO}_2@\text{TiO}_2$  microspheres through a wet-chemical approach. The  $\text{Fe}_3\text{O}_4@\text{SiO}_2@\text{TiO}_2$  microspheres possess both ferromagnetic and photocatalytic properties. The  $\text{TiO}_2$  nanoparticles on the surfaces of microspheres can degrade organic dyes under the illumination of UV light. Furthermore, the microspheres are easily separated from the solution after the photocatalytic process due to the ferromagnetic  $\text{Fe}_3\text{O}_4$  core. The photocatalysts can be recycled for further use with slightly lower photocatalytic efficiency.

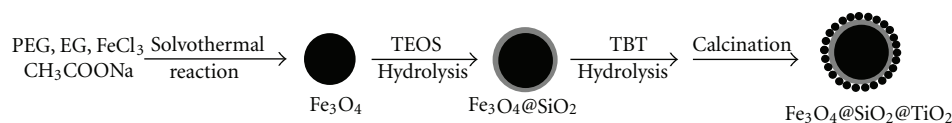
## 1. Introduction

In recent years, an enormous research effort has been dedicated to the study of semiconductors in the area of photocatalysis. Among the semiconductor photocatalysts,  $\text{TiO}_2$  has attracted a lot of attention because of its high photocatalytic efficiency, high stability, and low cost [1–5]. For the application of  $\text{TiO}_2$  in the area of wastewater purification,  $\text{TiO}_2$  slurry reactor is the most common device because of its high specific surface area, efficient light absorption, and good dispersion [6–8]. However, the separation of  $\text{TiO}_2$  particles from treated water, especially from a large volume of water, is an expensive and time-consuming work, which limited the application of  $\text{TiO}_2$  slurry reactor in industrial application. To solve this problem, many methods including titania beads [9],  $\text{TiO}_2$ -based thin film [10, 11], fiberglass loaded with titania [12], and encapsulated titania within a zeolite framework [13] have been developed to immobilize  $\text{TiO}_2$  in fixed beds. However, the photocatalytic activity of  $\text{TiO}_2$  is considerably reduced by these immobilization techniques because the effective surface area of photocatalysts is decreased.

Recently, magnetic core-shell composites have gained a great deal of attentions. The magnetic core has good magnetic responsibility and can be easily magnetized. Therefore,

the magnetic composites can be conveniently separated and collected from water by applying an external magnetic field. Many studies have been carried out on the preparation and application of  $\text{TiO}_2$ /magnetic composites [14–20]. In these studies,  $\text{Fe}_3\text{O}_4$  and  $\gamma\text{-Fe}_2\text{O}_3$  nanoparticles were applied as the core magnetic materials. However,  $\text{Fe}_3\text{O}_4$  nanoparticles are easily oxidized, even at room temperature. The  $\text{TiO}_2$  shell in the composites was usually prepared by sol-gel methods, where heat treatment was essential. After heat treatment, the ferromagnetic  $\gamma\text{-Fe}_2\text{O}_3$  may transform to paramagnetic  $\alpha\text{-Fe}_2\text{O}_3$ .

In this work, through the medium of  $\text{SiO}_2$ ,  $\text{TiO}_2$  nanoparticles were successfully coated on  $\text{Fe}_3\text{O}_4$  microspheres, and  $\text{Fe}_3\text{O}_4@\text{SiO}_2@\text{TiO}_2$  microspheres with well-defined core-shell structures were obtained. The prepared  $\text{Fe}_3\text{O}_4@\text{SiO}_2@\text{TiO}_2$  microspheres are multifunctional. The  $\text{TiO}_2$  nanoparticles are at the outmost of the core-shell microspheres, which can act as photocatalysts to decompose organic dyes in wastewater. The  $\text{Fe}_3\text{O}_4$  core makes them very easy to be separated and recycled from water with the help of an external magnet. Furthermore, the  $\text{Fe}_3\text{O}_4$  microspheres are stable at room temperature, and are unchanged after heat treatment under nitrogen atmosphere. Therefore, the  $\text{Fe}_3\text{O}_4@\text{SiO}_2@\text{TiO}_2$  microspheres may serve as an ideal photocatalyst for the treatment of wastewater.



SCHEME 1: The synthetic route to  $\text{Fe}_3\text{O}_4@\text{SiO}_2@\text{TiO}_2$  core-shell microspheres.

## 2. Experimental

All the chemical reagents were of analytical grade and were used without further purification.

**2.1. Synthesis of  $\text{Fe}_3\text{O}_4$  Microspheres.** The procedure for the synthesis of  $\text{Fe}_3\text{O}_4$  microspheres was carried out according to a previous report [21], summarized as follows: 1.35 g of iron chloride (III) hexahydrate, 1.0 g of polyethylene glycol ( $M_w = 4000$ ), and 3.6 g of sodium acetate trihydrate were added into 40 mL ethylene glycol under constant magnetic stirring to form a clear solution. Then the solution was transferred into a Teflon-lined stainless steel autoclave with a capacity of 50 mL and heated at  $180^\circ\text{C}$  for 19 h. The products were collected and fully rinsed with deionized water and absolute ethanol with the help of an external magnet, and then dried under vacuum at  $60^\circ\text{C}$  for 2 h for further use.

**2.2. Synthesis of  $\text{Fe}_3\text{O}_4@\text{SiO}_2$  Microspheres.** The synthesis of  $\text{Fe}_3\text{O}_4@\text{SiO}_2$  microspheres was carried out according to a previous report [22]. Typically, 0.2 g of as-prepared  $\text{Fe}_3\text{O}_4$  microspheres was dispersed into a mixture of 20 mL ethanol and 4 mL deionized water in a glass beaker, and then, under constant mechanical stirring, 1 mL of ammonia solution (25%) and 0.8 mL of tetraethyl orthosilicate (TEOS) were consecutively added. The mixture was further stirred for 3 h. The resultant products were collected and washed, and then dried under vacuum at  $60^\circ\text{C}$  for 2 h for further use.

**2.3. Synthesis of  $\text{Fe}_3\text{O}_4@\text{SiO}_2@\text{TiO}_2$  Microspheres.** The synthesis of  $\text{Fe}_3\text{O}_4@\text{SiO}_2@\text{TiO}_2$  microspheres was carried out according to following procedure. Firstly, 5 mL tetrabutyl titanate was dissolved in 35 mL ethanol to form a clear solution. Then, 0.1 g of  $\text{Fe}_3\text{O}_4@\text{SiO}_2$  microspheres as dispersed in the above solution with the aid of ultrasonication for 5 min. After that, 20 mL of a 1:5 (v/v) mixture of water and ethanol was added dropwise to the suspension of  $\text{Fe}_3\text{O}_4@\text{SiO}_2$  microspheres with constant mechanical stirring over a period of approximately 15 min. The suspension was further stirred for about 1 h. The products were collected and washed with ethanol for three times, then calcined under nitrogen atmosphere at  $500^\circ\text{C}$  for 3 h. The whole synthesis procedure is shown in Scheme 1.

**2.4. Photocatalytic Degradation of Methyl Orange.** The photocatalytic degradation was conducted as the following procedure: 40 mg of  $\text{Fe}_3\text{O}_4@\text{SiO}_2@\text{TiO}_2$  microspheres were dispersed into an aqueous solution of methyl orange ( $0.01\text{ g L}^{-1}$ , 50 mL). The pH value of the methyl orange solution was adjusted by hydrochloric acid and sodium hydroxide

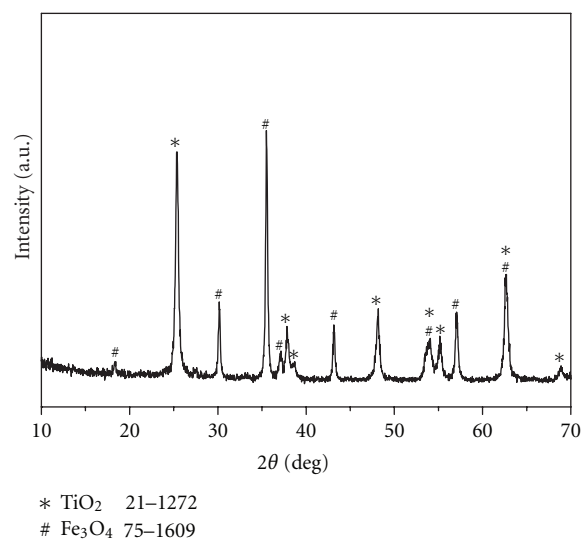


FIGURE 1: XRD pattern of the  $\text{Fe}_3\text{O}_4@\text{SiO}_2@\text{TiO}_2$  microspheres.

solution. Before photocatalytic experiments, the solution was stirred in the dark to permit the adsorption/desorption equilibrium until the concentration of methyl orange solution was constant. After that, a 300 W column-like low-pressure mercury lamp was placed over the solution with a distance of 20 cm, and the solution was irradiated with the lamp under constant mechanical stirring and fan cooling. At intervals of 10 min, 3 mL of the solution was taken out and analyzed with a UV-vis absorption spectrometer.

**2.5. Characterization.** X-ray powder diffraction (XRD) patterns were recorded using a Shimadzu XRD-6000 X-ray diffractometer equipped with graphite monochromatized  $\text{Cu K}\alpha$  radiation ( $\lambda = 0.15406\text{ nm}$ ). The field-emission scanning electron microscopy (FESEM) images were captured with a Hitachi S-4800 field-emission scanning electron microscope. Transmission electron microscopy (TEM) images were taken on a JEOL-2010 high-resolution transmission electron microscope. UV-vis absorption spectra were measured with a Shimadzu UV-3010 spectrometer.

## 3. Results and Discussion

The phase and composition of the as-obtained samples were examined by XRD. Figure 1 shows a typical XRD pattern of the  $\text{Fe}_3\text{O}_4@\text{SiO}_2@\text{TiO}_2$  microspheres. All of the diffraction peaks in this pattern can be classified into two sets. The peaks that marked with “#” can be indexed to the orthorhombic phase of  $\text{Fe}_3\text{O}_4$  (JCPDS card no. 75-1609), while the other

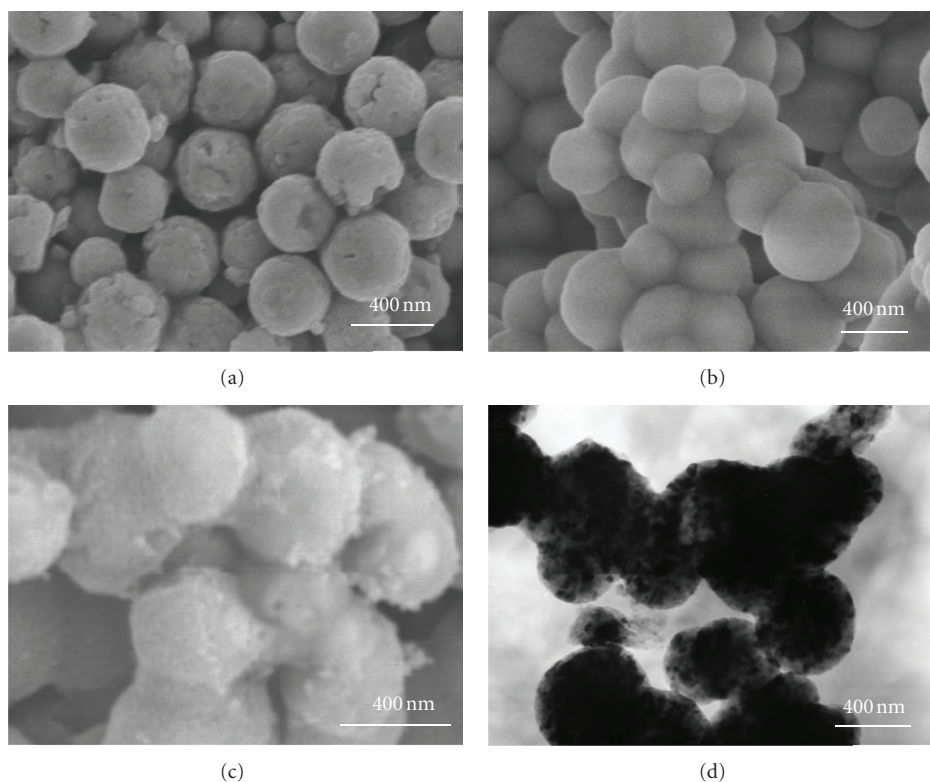


FIGURE 2: (a)–(c) FESEM images of the  $\text{Fe}_3\text{O}_4$  microspheres,  $\text{Fe}_3\text{O}_4@SiO_2$  microspheres, and  $\text{Fe}_3\text{O}_4@SiO_2@TiO_2$  microspheres, (d) TEM image of the  $\text{Fe}_3\text{O}_4@SiO_2@TiO_2$  microspheres.

peaks that marked with “\*” can be indexed to the tetragonal phase of  $TiO_2$  (JCPDS card no. 21–1272). No diffraction peaks corresponding to  $SiO_2$  were observed because the  $SiO_2$  is amorphous.

The morphology and size of the as-prepared products were characterized by FESEM and TEM. Figure 2(a) displays an FESEM image of the  $\text{Fe}_3\text{O}_4$  microspheres, in which many nearly monodisperse microspheres with diameters of about 400 nm can be seen. The surfaces of the  $\text{Fe}_3\text{O}_4$  microspheres are rough. Figure 2(b) shows an FESEM image of the  $\text{Fe}_3\text{O}_4@SiO_2$  microspheres. The surfaces of the  $\text{Fe}_3\text{O}_4@SiO_2$  microspheres are smooth, which is distinctly different from the initial  $\text{Fe}_3\text{O}_4$  microspheres that are shown in Figure 2(a). Such a difference can be attributed to the coating of  $SiO_2$  layer on  $\text{Fe}_3\text{O}_4$ . Figure 2(c) is an FESEM image of the  $\text{Fe}_3\text{O}_4@SiO_2@TiO_2$  microspheres, from which we can see that many tiny  $TiO_2$  nanoparticles with diameters of 10–20 nm are adhered to the  $SiO_2$  layer. Figure 2(d) is a TEM image of the  $\text{Fe}_3\text{O}_4@SiO_2@TiO_2$  microspheres, which shows many nanoparticles adhered to the microspheres, consistent with the FESEM observations.

Figure 3(a) shows a digital photograph of the  $\text{Fe}_3\text{O}_4@SiO_2@TiO_2$  microspheres that were dispersed in deionized water with the assistance of ultrasonication. The microspheres can be easily dispersed in water, and this suspension can be kept constant for several minutes. When a magnet was placed aside, the black microspheres can be quickly collected in several seconds, leaving a clear solution, as shown in

Figure 3(b). This result shows that the  $\text{Fe}_3\text{O}_4@SiO_2@TiO_2$  microspheres can be easily separated and collected from water with the assistance of external magnetic force.

The photocatalytic activities of the  $\text{Fe}_3\text{O}_4@SiO_2@TiO_2$  microspheres were investigated by photodegradation of methyl orange in aqueous solution under the irradiation of UV light. Figure 4 shows the time-dependent UV-vis absorption spectra of methyl orange aqueous solution ( $0.01 \text{ g L}^{-1}$ ,  $\text{pH} = 3$ ) in the presence of  $\text{Fe}_3\text{O}_4@SiO_2@TiO_2$  microspheres under exposure to UV light. The main absorption peak of methyl orange is centered at 506 nm. It is clear that the intensity of the main absorption peak of methyl orange gradually decreases with increasing time due to the concentration decreasing of methyl orange. This result shows that methyl orange is gradually degraded or changes into other structures under the irradiation of UV light in the presence of  $\text{Fe}_3\text{O}_4@SiO_2@TiO_2$  microspheres.

As a comparison, the photodegradation of methyl orange under different conditions was measured, as shown in Figure 5. When the reaction was carried out in the dark, there is hardly any degradation of methyl orange occurred. When  $\text{Fe}_3\text{O}_4@SiO_2@TiO_2$  microspheres were substituted by  $\text{Fe}_3\text{O}_4@SiO_2$  or  $\text{Fe}_3\text{O}_4$  microspheres, the degradation rate of methyl orange is dramatically decreased. This result shows that the  $TiO_2$  nanoparticles in the  $\text{Fe}_3\text{O}_4@SiO_2@TiO_2$  microspheres play key role in the photodegradation of methyl orange.

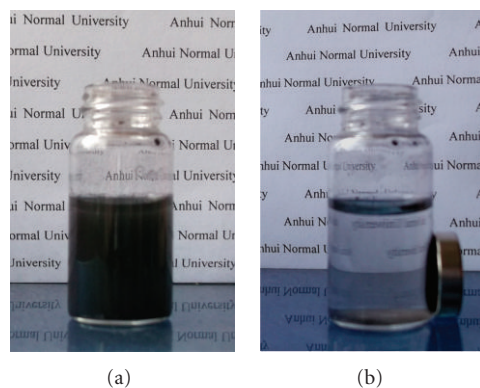


FIGURE 3: (a) Digital photograph of  $\text{Fe}_3\text{O}_4@\text{SiO}_2@\text{TiO}_2$  microspheres dispersed in water, (b) digital photograph of  $\text{Fe}_3\text{O}_4@\text{SiO}_2@\text{TiO}_2$  microspheres collected by an external magnet.

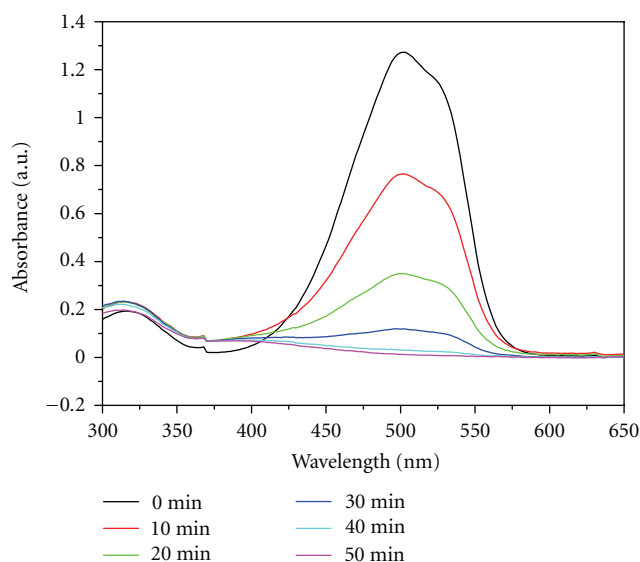


FIGURE 4: Time-dependent absorption spectra of a methyl orange aqueous solution ( $0.01 \text{ g L}^{-1}$ ,  $\text{pH} = 3$ ) in the presence of  $\text{Fe}_3\text{O}_4@\text{SiO}_2@\text{TiO}_2$  composites under exposure to UV light.

The pH value of solution is an important parameter in photocatalytic degradation reactions that are taking place on the surfaces of semiconductors. It dictates the surface charge properties of the photocatalyst and therefore the adsorption behavior of pollutants [23]. Here we examined the photocatalytic activities of the  $\text{Fe}_3\text{O}_4@\text{SiO}_2@\text{TiO}_2$  microspheres at different pH conditions. The results are shown in Figure 6. It is obvious that at acidic conditions the photocatalytic efficiency of the  $\text{Fe}_3\text{O}_4@\text{SiO}_2@\text{TiO}_2$  microspheres is much higher, and the photocatalytic efficiency decreases with the increase of pH value. At acidic conditions, the surface of  $\text{TiO}_2$  will be positively charged, so the negatively charged dye anion can be effectively adsorbed, and higher photocatalytic efficiency is obtained.

The  $\text{Fe}_3\text{O}_4@\text{SiO}_2@\text{TiO}_2$  microspheres can be conveniently separated and collected from the treated water after

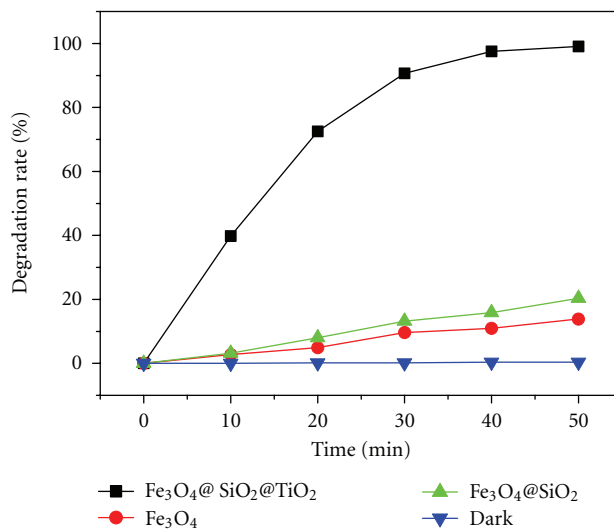


FIGURE 5: Degradation rate of methyl orange aqueous solution in the dark or in the presence of different photocatalyst under exposure to UV light.

photocatalytic reactions are completed; therefore, they can be recycled for further use. Here we studied the photocatalytic efficiency of the  $\text{Fe}_3\text{O}_4@\text{SiO}_2@\text{TiO}_2$  microspheres for recyclable usage. Figure 7 shows the photocatalytic efficiency of the  $\text{Fe}_3\text{O}_4@\text{SiO}_2@\text{TiO}_2$  microspheres after 6 cycles. In each cycle, the methyl orange solution ( $0.01 \text{ g L}^{-1}$ ,  $\text{pH} = 3$ ) was irradiated under UV light for 45 min. The results show that the photocatalytic activity of the  $\text{Fe}_3\text{O}_4@\text{SiO}_2@\text{TiO}_2$  microspheres only decreased a little after 6 cycles of the photocatalysis experiments. The reason may be that some of the  $\text{TiO}_2$  nanoparticles are broken away from the  $\text{Fe}_3\text{O}_4@\text{SiO}_2@\text{TiO}_2$  microspheres when they are stirred; as a result, the photocatalytic efficiency of the  $\text{Fe}_3\text{O}_4@\text{SiO}_2@\text{TiO}_2$  microspheres decreases. However, the degradation rate of methyl orange can still reach 91% after 6 cycles of reuse. So the  $\text{Fe}_3\text{O}_4@\text{SiO}_2@\text{TiO}_2$  microspheres can be applied as recyclable photocatalysts.

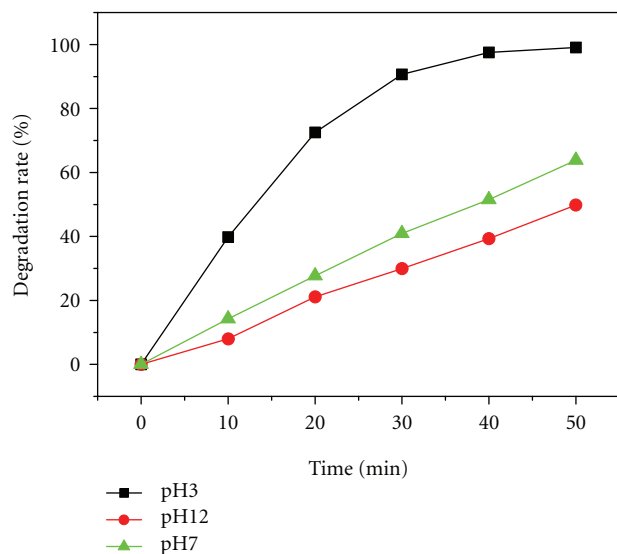


FIGURE 6: Degradation rate of methyl orange aqueous solution at different pH values in the presence of  $\text{Fe}_3\text{O}_4@\text{SiO}_2@\text{TiO}_2$  composites under exposure to UV light.

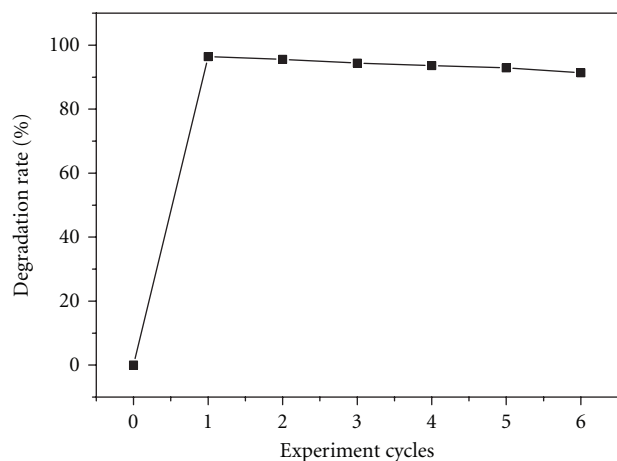


FIGURE 7: Relationship between the degradation efficiency of  $\text{Fe}_3\text{O}_4@\text{SiO}_2@\text{TiO}_2$  photocatalyst and cyclic time.

#### 4. Conclusions

In summary, we have successfully prepared  $\text{Fe}_3\text{O}_4@\text{SiO}_2@\text{TiO}_2$  microspheres with well-defined core-shell structures through a wet-chemical method. The  $\text{Fe}_3\text{O}_4@\text{SiO}_2@\text{TiO}_2$  microspheres are multifunctional. The magnetic core makes the microspheres very easy to be separated from solution with the help of an external magnet, and the titania nanoparticles at the outside can act as photocatalyst to decompose organic dyes in waste water. Photocatalytic experiments show that the prepared  $\text{Fe}_3\text{O}_4@\text{SiO}_2@\text{TiO}_2$  microspheres have good photocatalytic activities under the illumination of UV light and can be applied as recyclable photocatalysts.

#### Acknowledgment

Financial supports from the National Natural Science Foundation of China (20701001, 21171006) are gratefully acknowledged.

#### References

- [1] A. Fujishima and K. Honda, "Electrochemical photolysis of water at a semiconductor electrode," *Nature*, vol. 238, no. 5358, pp. 37–38, 1972.
- [2] M. R. Hoffmann, S. T. Martin, W. Choi, and D. W. Bahnemann, "Environmental applications of semiconductor photocatalysis," *Chemical Reviews*, vol. 95, no. 1, pp. 69–96, 1995.
- [3] A. Wold, "Photocatalytic properties of  $\text{TiO}_2$ ," *Chemistry of Materials*, vol. 5, no. 3, pp. 280–283, 1993.
- [4] H. Park and W. Choi, "Effects of  $\text{TiO}_2$  surface fluorination on photocatalytic reactions and photoelectrochemical behaviors," *Journal of Physical Chemistry B*, vol. 108, no. 13, pp. 4086–4093, 2004.
- [5] V. A. Sakkas, A. Dimou, K. Pitarakis, G. Mantis, and T. Albanis, " $\text{TiO}_2$  photocatalyzed degradation of diazinon in an aqueous medium," *Environmental Chemistry Letters*, vol. 3, no. 2, pp. 57–61, 2005.
- [6] K. W. Kim, S. H. You, S. S. Park, G. H. Kang, W. T. Bae, and D. W. Shin, "Effect of experimental conditions on photocatalytic efficiency in  $\text{TiO}_2$  powder slurry systems," *Journal of Ceramic Processing Research*, vol. 9, no. 5, pp. 530–537, 2008.
- [7] I. Arslan, I. A. Balcioglu, and D. W. Bahnemann, "Heterogeneous photocatalytic treatment of simulated dyehouse effluents using novel  $\text{TiO}_2$ -photocatalysts," *Applied Catalysis B*, vol. 26, no. 3, pp. 193–206, 2000.
- [8] N. Bouanimba, R. Zouaghi, N. Laid, and T. Sehili, "Factors influencing the photocatalytic decolorization of Bromophenol blue in aqueous solution with different types of  $\text{TiO}_2$  as photocatalysts," *Desalination*, vol. 275, no. 1–3, pp. 224–230, 2011.
- [9] S. Yamazaki, S. Matsunaga, and K. Hori, "Photocatalytic degradation of trichloroethylene in water using  $\text{TiO}_2$  pellets," *Water Research*, vol. 35, no. 4, pp. 1022–1028, 2001.
- [10] H. Kominami, H. Kumamoto, Y. Kera, and B. Ohtani, "Immobilization of highly active titanium(IV) oxide particles: A novel strategy of preparation of transparent photocatalytic coatings," *Applied Catalysis B*, vol. 30, no. 3–4, pp. 329–335, 2001.
- [11] I. M. Arabatzis, S. Antonaraki, T. Stergiopoulos et al., "Preparation, characterization and photocatalytic activity of nanocrystalline thin film  $\text{TiO}_2$  catalysts towards 3,5-dichlorophenol degradation," *Journal of Photochemistry and Photobiology A*, vol. 149, no. 1–3, pp. 237–245, 2002.
- [12] S. Horikoshi, N. Watanabe, H. Onishi, H. Hidaka, and N. Serpone, "Photodecomposition of a nonylphenol polyethoxylate surfactant in a cylindrical photoreactor with  $\text{TiO}_2$  immobilized fiberglass cloth," *Applied Catalysis B*, vol. 37, no. 2, pp. 117–129, 2002.
- [13] M. Anpo, S. G. Zhang, H. Mishima, M. Matsuoka, and H. Yamashita, "Design of photocatalysts encapsulated within the zeolite framework and cavities for the decomposition of NO into  $\text{N}_2$  and  $\text{O}_2$  at normal temperature," *Catalysis Today*, vol. 39, no. 3, pp. 159–168, 1997.
- [14] D. Beydoun, R. Amal, G. K. C. Low, and S. McEvoy, "Novel photocatalyst: titania-coated magnetite. Activity and

- photodissolution,” *Journal of Physical Chemistry B*, vol. 104, no. 18, pp. 4387–4396, 2000.
- [15] D. Beydoun, R. Amal, J. Scott, G. Low, and S. McEvoy, “Studies on the mineralization and separation efficiencies of a magnetic photocatalyst,” *Chemical Engineering & Technology*, vol. 24, no. 7, pp. 745–748, 2001.
- [16] F. Chen, Y. Xie, J. Zhao, and G. Lu, “Photocatalytic degradation of dyes on a magnetically separated photocatalyst under visible and UV irradiation,” *Chemosphere*, vol. 44, no. 5, pp. 1159–1168, 2001.
- [17] D. Beydoun and R. Amal, “Implications of heat treatment on the properties of a magnetic iron oxide-titanium dioxide photocatalyst,” *Materials Science and Engineering B*, vol. 94, no. 1, pp. 71–81, 2002.
- [18] Y. Gao, B. Chen, H. Li, and Y. Ma, “Preparation and characterization of a magnetically separated photocatalyst and its catalytic properties,” *Materials Chemistry and Physics*, vol. 80, no. 1, pp. 348–355, 2003.
- [19] W. Wu, X. H. Xiao, S. F. Zhang, F. Ren, and C. Z. Jiang, “Facile method to synthesize magnetic iron oxides/TiO<sub>2</sub> hybrid nanoparticles and their photodegradation application of methylene blue,” *Nanoscale Research Letters*, vol. 6, no. 1, p. 533, 2011.
- [20] C. F. Chang and C. Y. Man, “Titania-coated magnetic composites as photocatalysts for phthalate photodegradation,” *Industrial & Engineering Chemistry Research*, vol. 50, no. 20, pp. 11620–11627, 2011.
- [21] H. Deng, X. Li, Q. Peng, X. Wang, J. Chen, and Y. Li, “Monodisperse magnetic single-crystal ferrite microspheres,” *Angewandte Chemie*, vol. 44, no. 18, pp. 2782–2785, 2005.
- [22] W. Stöber, A. Fink, and E. Bohn, “Controlled growth of monodisperse silica spheres in the micron size range,” *Journal of Colloid And Interface Science*, vol. 26, no. 1, pp. 62–69, 1968.
- [23] V. K. Gupta, R. Jain, A. Mittal et al., “Photo-catalytic degradation of toxic dye amaranth on TiO<sub>2</sub>/UV in aqueous suspensions,” *Materials Science and Engineering C*, vol. 32, no. 1, pp. 12–17, 2012.



# Hindawi

Submit your manuscripts at  
<http://www.hindawi.com>

